Ti targets, which could be due principally to uncertainties in the cross section measurements. Errors in the cross-section measurements for the light element targets are less than 20%, but for Ti, Co, and Cu could be as high as 40%. Small amounts of light element impurities in these targets are possible, a problem particularly unavoidable in the metallurgical processing of

Ti, and the surface oxide also contributes to the total Be^7 yield from the $O^{16}(\text{He}^4,\text{Be}^7)$ reaction.

ACKNOWLEDGMENT

Photoneutron Cross-Section Measurements on Gold Using nearly Monochromatic Photons*

S. C. Fultz, R. L. Bramblett, J. T. Caldwell, and N. A. Kerr

Lawrence Radiation Laboratory, University of California, Livermore, California

(Received April 9, 1962)

Continuously variable monochromatic gamma rays with an energy spread of 3% have been produced using the annihilation in flight of positrons accelerated in a linear electron accelerator. These gamma rays have been employed to measure the (γ,n) and $(\gamma,2n)$ cross sections for gold. A neutron counting method was used to determine the neutron multiplicity. The photoneutron yield for Au has a maximum of 535 ± 37 mb at 13.7 ± 0.3 MeV. The $(\gamma,2n)$ cross section was observed to have a threshold at 14.5 ± 0.5 MeV and a maximum of approximately 100 mb at 18 MeV. The integrated (γ,n) and $(\gamma,2n)$ cross sections, up to 25 MeV, were found to be 2.14 ± 0.15 and 0.83 ± 0.16 MeV-b, respectively. The value of $\int_0^\infty \sigma E^{-2} dE$ was determined to be 15.3 ± 1.5 mb/MeV. The level density parameter a was found to be 17.1 ± 0.5 MeV^{-1}. The total cross section $\sigma(\gamma,n)+\sigma(\gamma,2n)+\sigma(\gamma,pn)$ can be fitted with a single Lorentz curve having a peak cross section of 535 mb at 13.90 MeV and a width of 4.2 MeV.

INTRODUCTION

CROSS-SECTION measurements for nuclear photo-disintegration have been undertaken in recent years by use of several sources of gamma rays. These include monochromatic gamma rays obtained from radioactive sources or charged-particle reactions, and continuous bremsstrahlung from betatrons.[1] All three have disadvantages. The photon energies available from radioactive sources are low, which greatly limits the scope of photonuclear studies made by their use. Gamma rays from charged-particle reactions are obtainable with energies up to about 20 MeV, but they are usually discrete or in some cases have a limited range of variability and are of low intensity. Most photonuclear studies have been made by use of electron bremsstrahlung produced by betatrons. The betatron energy can be accurately controlled and is continuously variable. However, the bremsstrahlung is continuous in distribution up to the energy of the electrons and has its greatest intensity at low energies. Because of the continuous nature of the bremsstrahlung spectrum, the reduction of photonuclear data consists of a complex unfolding procedure in order to reduce a yield curve to an excitation function for the reaction being studied. Since the yield curves have a small slope on the high

side of the giant resonance, the analysis involves taking small differences between large numbers, which leads to large uncertainties and sources of error which are difficult to evaluate. In order to determine the formation cross section, the multiplicity of neutrons above the $(\gamma,2n)$ and $(\gamma,3n)$ thresholds must be known. These have been determined only in a few cases—by measuring radioactivity induced in the sample materials. This procedure, however, compounds the errors of activation analysis with those of unfolding bremsstrahlung. Some attempts have been made to calculate the multiplicity, but such calculations are subject to large errors.

The method described below for measuring photoneutron cross sections overcomes many of the disadvantages of the techniques commonly used. It consists of employing essentially monochromatic photons of variable energy as the source of gamma radiation. The monochromatic photons are created through the annihilation in flight of a beam of monoenergetic fast positrons. In addition, multiplicities of neutrons are determined experimentally, thus making possible determination of (γ,n) and $(\gamma,2n)$ cross sections.

EXPERIMENTAL EQUIPMENT AND METHOD

A 22-MeV, high-current, linear electron accelerator[2] has been used to produce positrons through pair

---

[1] M. Elaine Toms, "Bibliography of Photonuclear Reactions," U. S. Naval Research Laboratory, 1960 (unpublished).

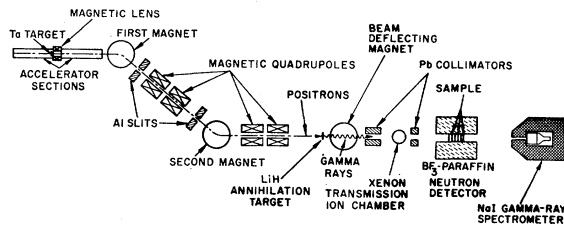[2] N. A. Austin and S. C. Fultz, Rev. Sci. Instr. **30**, 284 (1959).

FIG. 1. Experimental apparatus for photoneutron cross-section measurements. The drawing is not to scale. Neutron shields and some gamma-ray shielding have been omitted.

production in a heavy-element target.[3] Magnetic analysis yields a beam of nearly monoenergetic positrons. When these are made to pass through target material of low atomic number (the annihilation target), they annihilate in flight with electrons in the target material. In doing so, photons moving in the forward direction carry off the energy of the mono-energetic positrons. Hence, it is possible to produce a beam of nearly monochromatic photons in the forward direction. By continuously varying the energy of the positrons, this photon beam can also be made continuously variable in energy.

The equipment used for the experiments described below is shown in Fig. 1. The positrons were produced in a 0.10-in.-thick tantalum or tungsten target which was inserted between the first and second sections of the accelerator. The target was water cooled and was positioned close to the end of the first accelerator section. It was immediately followed by a magnetic lens which served to focus positrons into the entrance aperture of the second section. Positrons entering the second accelerator section were accelerated by operating it with the radio frequency 180° out of phase with that of the first section. The energy of the accelerated positrons was controlled by regulating the phase and power of the radio frequency in the second section in addition to regulating the current through the bending magnets. The positrons were created by pair production from bremsstrahlung arising from 10-MeV electrons incident on the thick tungsten target. The choice of low electron energy for the creation of pairs minimized the background arising from neutrons since the maximum energy of the bremsstrahlung was close to threshold for the (γ,n) reaction in the target material. In addition, the relatively low bremsstrahlung energy was easily shielded out of the gamma detection system, thus reducing to a negligible magnitude all backgrounds originating from the accelerator.

The positron beam emerging from the accelerator was then energy-analyzed by passing it through an analyzing magnet and a two-jaw slit. The slit width was set at approximately 0.25 in., corresponding to a momentum resolution of about 3%. After passing through the slit the diverging beam was focused by use

of a pair of quadrupole magnets and made to pass through a four-jaw aluminum slit. It then passed through a second magnet and was deflected along a line parallel to its original direction. After passing through the second magnet, it was made to pass through a second pair of quadrupoles which focused the beam onto an annihilation target of low-atomic-number material such as Be or LiH. Those positrons not stopped in the annihilation target were swept out of the line of sight of the gamma-ray monitors and sample by the field of a 2-kW magnet. The photons created by the annihilation in flight of the positrons passed through a 6-in.-thick lead collimator with an aperture of about 1.5-in. diam, and through a transmission ion chamber and a second collimator, before striking the sample being irradiated. The energy resolution of the photons was measured by use of the 15.1-MeV gamma rays obtained from annihilation-photon excitation of the 15.1-MeV level in C^{12}. It was found to be about 3%, which can be mostly attributed to the momentum resolution of the magnetic analyzer.[4] The energy of the annihilation photons was 0.76 MeV higher than that of the positrons for most of the measurements described below.

A 6 in. long by 5-in. diam NaI(Tl) crystal spectrometer was set up on the line of sight along the direction of the positrons incident on the annihilation target. It measured gamma spectra transmitted through a 3-in.-diam axial hole in the neutron detector, both when the sample was located in the detector and when it was absent. The true number of monochromatic photons was found by taking the area under the peak of the pulse-height spectrum, and adding a correction for the tail of low-amplitude pulses.[5] A typical pulse-height spectrum for radiations emitted from a LiH target is given in Fig. 2. The rise in the distribution of pulses in the regions of small amplitude is attributable to the continuous positron bremsstrahlung.
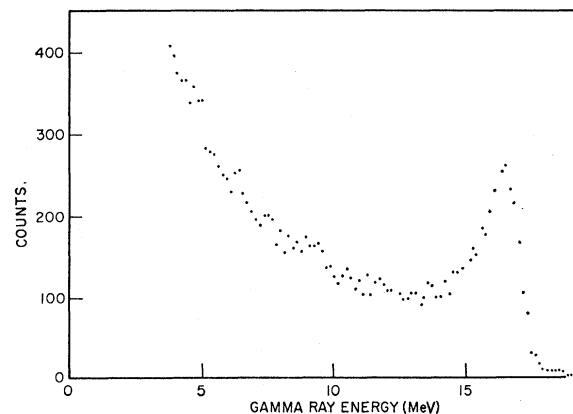

FIG. 2. Pulse-height spectrum of gamma rays from 15.6-MeV positrons incident on a 0.060-in. thick LiH target.

[3] C. P. Jupiter, N. E. Hansen, R. E. Shafer, and S. C. Fultz, Phys. Rev. 121, 866 (1961).

[4] C. R. Hatcher, R. L. Bramblett, N. E. Hansen, and S. C. Fultz, Nuclear Instr. & Methods 14, 337 (1961).

[5] J. Kockum & N. Starfelt, Nuclear Instr. & Methods 4, 171 (1959).

The transmission ion chamber consisted of a 1-liter spherical steel chamber filled with xenon to a pressure of 1 atm. It served the valuable function of a gamma-ray monitor having substantial dynamic range, and thus circumvented the problem of pulse pileup which is frequently encountered in large-crystal gamma-ray spectrometers. The ion chamber was calibrated by correlating the charge collected from it to the spectrum seen by the gamma-ray spectrometer, for positrons of various energies incident on the annihilation target. A typical calibration curve for the xenon ion chamber is given in Fig. 3.

The sample usually consisted of a number of 0.25 in. thick by 2-in. diam disks of material which were located at the center of an 18-in. cubic 4π paraffin-moderated neutron detector, inserted through an axial channel in the paraffin cube. The detectors consisted of 24 high-pressure BF_3 counters which were arranged in concentric circles about the axial hole. The minimum web thickness of paraffin between the central aperture and the first ring of BF_3 counters was adjusted so that the counter exhibited essentially the same sensitivity to neutrons having average energies of 25 keV, 1.2 MeV, and 2 MeV. The detector efficiency was therefore considered to be constant over the range of neutron energies expected.

The procedure followed in the process of making measurements on photoneutron cross sections consisted of measuring neutrons and photons simultaneously for a selected positron energy. The positron energy was then changed, and the measurements were repeated. The procedure was repeated until the desired range of positron energies was covered. The magnetic fields of all magnets were then reversed, and the negative parts of the pairs produced in the bremsstrahlung target were selected. This made available a beam of negative electrons similar in intensity to that of the positrons. For each selected energy of negative electrons, simultaneous measurements on neutrons and photons were
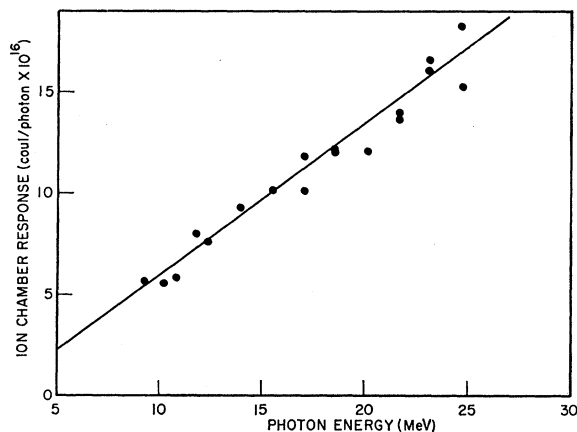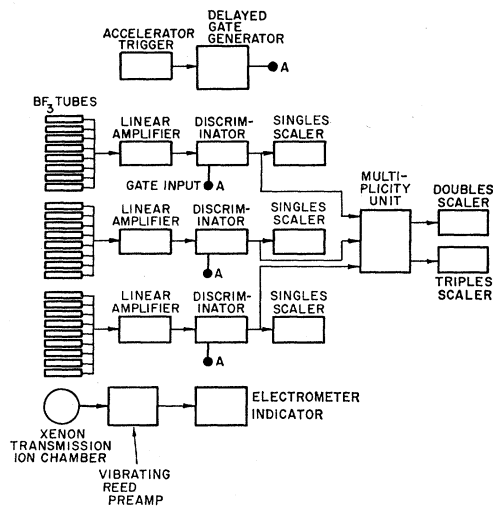

FIG. 4. Block diagram of the electronic circuitry employed for the photoneutron cross-section measurements.

again made. The procedure was repeated until a range of energies corresponding to those examined by use of the positrons had been covered. The neutron yields obtained by use of the negative electrons were characteristic of those obtained with continuous bremsstrahlung radiation. They were normalized to the positron bremsstrahlung, for similar positron energies, and subtracted from the positron data. In this manner, positron data were corrected for the contributions from the positron bremsstrahlung, and the corrected yields were thus attributed to the nearly monochromatic annihilation photons.

The procedure outlined above was applied to all types of neutron data observed. In general, three types of neutron data were recorded:

(a) All the neutrons detected during each beam pulse were counted in scaling circuits designated as "singles" scalers.

(b) All cases where two or more neutrons were recorded per beam pulse were registered on a scaling circuit designated the "doubles" scaler.

(c) All cases where three or more neutrons were recorded per beam pulse were registered on a scaling circuit designated as the "triples" scaler.

The single-neutron count rate was proportional to the efficiency ϵ of the 4π neutron detector, which was 0.17. The double count rate was proportional to the square of the detector efficiency (ϵ^2), while the triple count rate was proportional to the cube of the detector efficiency (ϵ^3). For the cases examined, the efficiency of the neutron detector was insufficient to give reliable triples data. In addition, the energy of photons available seldom went much beyond the calculated $\sigma(\gamma,3n)$ threshold.

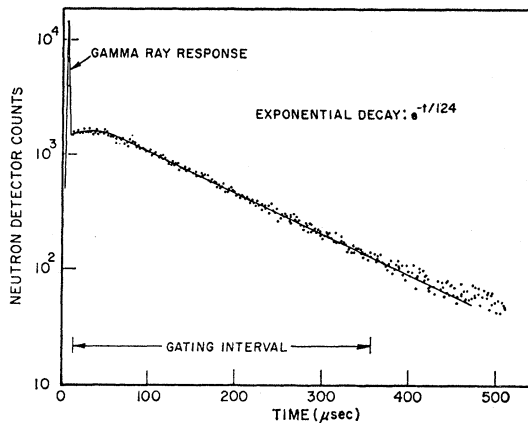The neutron data were recorded as single, double, or triple counts per beam pulse. The contributions to the

FIG. 3. Typical calibration curve for the 1-liter xenon-filled transmission ion chamber. The charge collected per photon is in units of 10^{-16} C.

FIG. 5. The characteristic time response curve for the 4π paraffin-moderated neutron detector. The decay period for neutrons was 124 μsec. The sharp peak at the beginning of the curve arises from the response of the BF_3 tubes to the gamma rays.

counts of one multiplicity had to be corrected for the random overlap of counts arising from nuclear events of other multiplicities.[6] For example, the doubles counts were corrected for the random occurrence of two single counts, during the gate time, or of one count from a single event and one from a triple event, etc. A statistical analysis was therefore applied to all multiplicity data, and for this the highest multiplicity considered was three neutrons emitted per nuclear event.

The cross sections were calculated by use of the expression

$$\sigma(\gamma,in) = (N_i/A)(\Omega_\gamma/\Omega_s)\mu/(1-e^{-\mu t})\epsilon_n{}^i N_a,$$

where i denotes the multiplicity, N_i is the number of neutron counts of multiplicity i, A denotes the number of annihilation photons detected, μ is the absorption coefficient in the sample for the nearly monoenergetic photons, t is the thickness of the sample, $\epsilon_n{}^i$ is the efficiency of the neutron counter raised to the power of the multiplicity, N_a is the number of atoms of sample material per cm^3, and Ω_γ/Ω_s is the ratio of solid angles subtended at the gamma spectrometer and at the sample, from the annihilation target.

Figure 4 shows a block diagram of the electronic circuitry employed for the cross-section measurements. The gamma detector, i.e., the transmission Xe ion chamber, was in operation for the duration of each run. The neutron counters, however, were gated "on" only after a suitable delay after the gamma-ray burst, and remained on for à period of 335 μsec. The delay was needed to wait out effects of the gamma-ray burst on the BF_3 detector tubes, since the tubes are moderately sensitive to gamma rays. The decay period for the neutron detector was 124 μsec. The function of the "multiplicity unit" was to mix all signals from all

[6] V. J. Ashby, H. C. Catron, L. L. Newkirk, and C. J. Taylor, Phys. Rev. 111, 616 (1958).

neutron detectors, and sort out those cases where double or triple neutron counts per beam burst occurred. The characteristic time-response curve for the neutron detector is given in Fig. 5. The short-period peak at the front of the curve represents the response to the gamma rays.

RESULTS FOR GOLD

For the photoneutron cross-section measurements on gold, the sample consisted of one to four 2-in.-diam disks, each about 0.25 in. thick. They were mounted in a thin cylinder of plastic foam, to give the desired mechanical rigidity, and were inserted into the center of the 3-in.-diam axial hole in the paraffin-moderated neutron detector. The neutron detector was calibrated twice daily with a standard mock-fission neutron source, while the ion chamber efficiency was similarly checked by use of a standardized Na^{22} source.

Measurements were made on the neutron yield and integrated gamma rays for a number of chosen positron and negative electron energies, ranging from 8.5 to 24 MeV. A typical set of data, partially reduced, is given in Fig. 6. Here can be seen neutron yields obtained by the use of positrons and negative electrons for the cases where one and two neutrons were detected per beam pulse. For each case, the upper curve was obtained from positron data while the lower curve was obtained from negative electron data. The difference between the two curves is proportional to the sum of partial cross sections for the interaction of nearly monochromatic gamma rays with gold nuclei. It can be seen that the shape of the giant resonance is immediately apparent in the positron data, while the negative
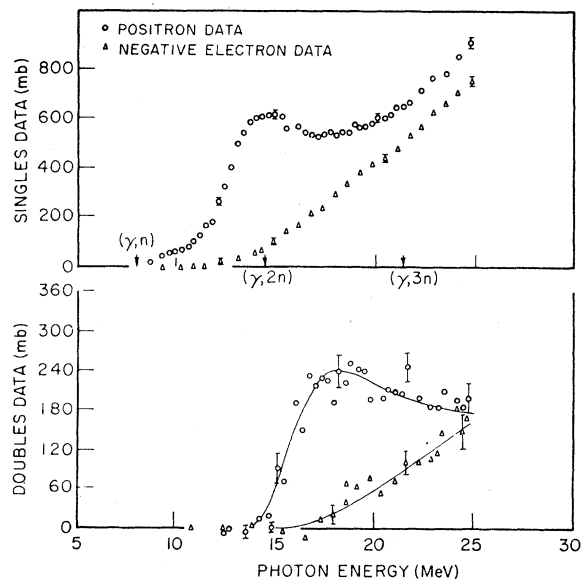

FIG. 6. Partially reduced neutron yield curves for Au. The top set was obtained from counting single neutrons per beam pulse, the lower set from counting two neutrons per beam pulse. For each set of curves, the top curve was obtained by use of positrons while the lower curve was obtained by use of negative electrons.
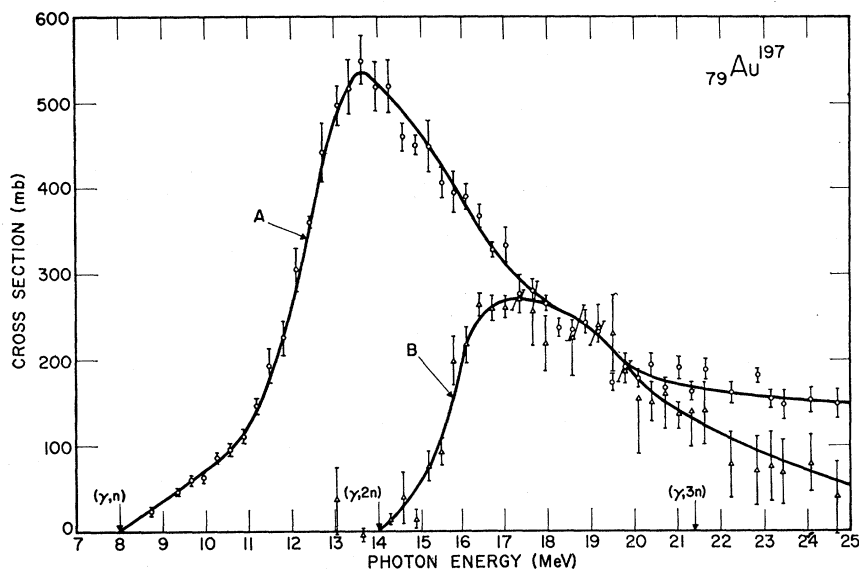
FIG. 7. Cross section obtained from neutron yield data. The top curve (A) consists of $\sigma(\gamma,n)$ $+2\sigma(\gamma,2n)+\sigma(\gamma,np)+3\sigma(\gamma,3n)$ and was obtained from single-neutron counting data. The lower curve (B) was obtained from double-neutron counting data and consists of $2\sigma(\gamma,2n)+6\sigma(\gamma,3n)$.

electron data are similar to the yield curves obtained by the use of betatrons as a source of radiation. The data agree well with the (γ,n) and $(\gamma,2n)$ thresholds calculated from mass data,[7] which are at 8.07 and 14.47 MeV, respectively.

A plot of the data, after reduction to cross sections, is given in Fig. 7. The upper curve represents a combination of several partial cross sections, i.e., $\sigma(\gamma,n)+\sigma(\gamma,pn)+2\sigma(\gamma,2n)+3\sigma(\gamma,3n)$, and was obtained from analysis of the single-neutron counting data. The lower curve is a plot of twice the cross section obtained from reduction of the double-neutron counting data, and includes $2\sigma(\gamma,2n)+6\sigma(\gamma,3n)$. The efficiency of the detector was too low to obtain reliable triple-neutron counting data. Consequently, the triples data were neglected. The apparent increase of the singles data over the doubles data at high energy can probably be attributed to uncertainty in the neutron counter efficiency and to errors in the multiplicity calculation. Another possibility is that a substantial amount of direct interaction sets in at this energy region.

Note added in proof.—Further measurements were recently made in the energy range from 19 to 25 MeV under improved experimental conditions. Results show that the top curve in Fig. 7 should coincide with the lower curve, for the energy range from 20 to 25 MeV. This yields integrated cross-section values up to 25 MeV of 2.14+0.15 and 0.83±0.16 MeV-b for $\sigma(\gamma,n)$ and $\sigma(\gamma,2n)$, respectively. These values have been corrected in the text of the report. A slight correction (1 or 2%) to the integrated cross section would account for the $\sigma(\gamma,3n)$ contribution. The $\sigma(\gamma,n)$ and $\sigma(\gamma,2n)$ curves are shown in Fig. 8. To obtain these curves, the $2\sigma(\gamma,2n)$ curve of Fig. 7 was subtracted from the total-cross- section curve to give $\sigma(\gamma,n)+\sigma(\gamma,np)$. The lower curve

represents the sum $\sigma(\gamma,2n)+3\sigma(\gamma,3n)$. The nuclear-formation cross section shown in Fig. 9 is the sum of the cross-section data given in Fig. 8. This contains the sum of the partial cross sections $\sigma(\gamma,n)+\sigma(\gamma,2n)+\sigma(\gamma,np)$. The solid curve is a Lorentz fit to the data.

A possible source of error in the neutron measurements could arise from the self-absorption of neutrons in the thick gold sample. In order to measure this effect, the sample thickness was reduced by factors of two and four and the cross-section measurements were repeated. No measurable effect was observed when the gold sample was reduced from 44 g/cm^2 to 11 g/cm^2. An additional check on self-absorption was made by measuring the count rate of the neutron detector for a mock-fission source: (a) when the source was in the presence of the gold sample, and (b) when the source was alone in the detector. Again no measurable effect was found. It was therefore concluded that no measurable self-absorption effect was present in the observed neutron-yield data.

Errors in the cross-section calculations arising from counting statistics were ±7%. The efficiency of the detector was determined to ±5%, and statistical errors in the calibration of the ion chamber were approximately ±5%. Hence, the net error in the cross-section determination is assumed to be approximately 10%. This error would apply to the integrated cross sections and minus-second cross section discussed below.

DISCUSSION AND CONCLUSIONS

Gold has been investigated by use of bremsstrahlung radiation in several previous instances. Fuller and Weiss[8] obtained a peak cross section of 590 mb at about 13.5 MeV. The width at half maximum (Γ) was about 4.5 MeV. They obtained an integrated cross section

[7] L. A. Koenig and J. H. E. Mattauch, *Nuclear Data Tables* (U. S. Atomic Energy Commission, Washington, D. C., 1960).
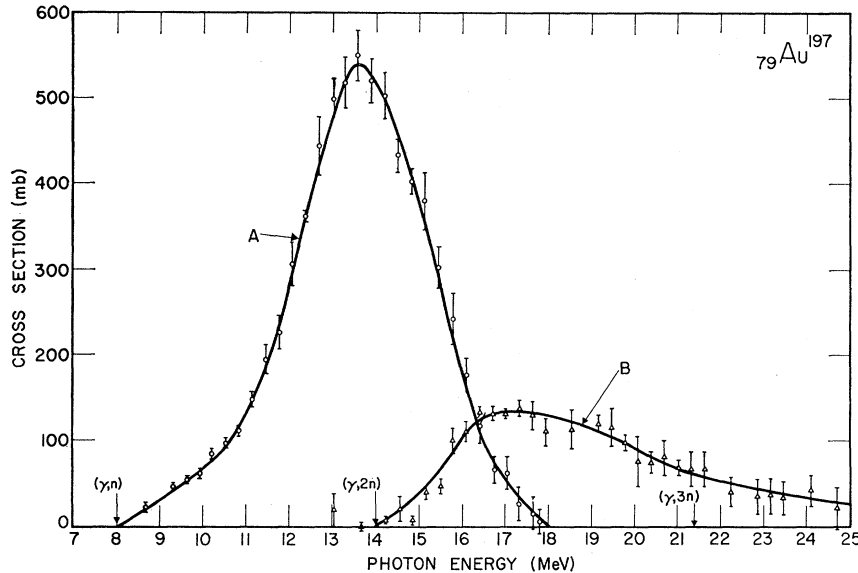
[8] E. G. Fuller and M. S. Weiss, Phys. Rev. 112, 560 (1958).

FIG. 8. Partial cross-section curves for gold. Curve A consists of $\sigma(\gamma,n)+\sigma(\gamma,np)$. Curve B consists of $\sigma(\gamma,2n)+3\sigma(\gamma,3n)$.

(up to 24 MeV) of approximately 3.47 MeV-b. Nathans and Halpern[9] obtained a peak cross section of 456 mb at approximately 14 MeV, with a Γ value of 6.9 MeV and an integrated cross-section value of 3.19 MeV-b. Montalbetti, Katz, and Goldemberg[10] give a peak cross section of 700 mb at 14.2 MeV with a Γ of 6.3 MeV and an integrated cross section of about 4.6 MeV-b [includes $\sigma(\gamma,n)+\sigma(\gamma,np)+2\sigma(\gamma,2n)$]. More recently, Nascimento, Moscati, and Goldemberg[11] have measured (γ,n) and $(\gamma,2n)$ cross sections for gold. The data yield a peak cross section of approximately 540 mb at 14.5 MeV with (γ,n) and $(\gamma,2n)$ integrated cross sections of approximately 3.45 and 1.24 MeV-b.

From the data obtained during the present experiment the following information has been derived. The integrated cross sections for $\sigma(\gamma,n)+\sigma(\gamma,np)$ and $\sigma(\gamma,2n)$ up to 25 MeV are 2.14±0.15 and 0.83±0.16 MeV-b, respectively. Hence, about 28% of the integrated cross section can be attributed to $\sigma(\gamma,2n)$. The total integrated cross section is 2.97±0.31 MeV-b. This is in reasonable agreement with the value deduced from the Thomas-Reiche-Kuhn sum rule,

$$\sigma_{\text{int}}=\int_0^\infty \sigma dE=0.06\frac{NZ}{A}=2.84 \text{ MeV-b.} \qquad (1)$$

The "minus-second cross section" σ_{-2} computed by Migdal[12] was also deduced from the data obtained.

$$\sigma_{-2}=\int_0^\infty \sigma E^{-2}dE=2.25A^{5/3} \mu\text{b/MeV.} \qquad (2)$$

For gold the experimental value of the "minus-second cross section" was found to be 15.3±1.5 mb/MeV. This compares favorably with the calculated value of 14.85 mb/MeV.

From the $\sigma(\gamma,2n)$ curve (Fig. 8) and the formation cross section (Fig. 9) can be obtained the ratio of $\sigma(\gamma,2n)$ to the total cross section. This ratio has been derived theoretically by Weisskopf,[13] assuming a Fermi gas behavior of the nucleons, and is given by

$$\sigma(\gamma,2n)/\sigma_{\text{tot}}=1-[1+(\epsilon_c/\theta)]\exp[-\epsilon_c/\theta], \qquad (3)$$

where ϵ_c is the excess energy over the threshold for the $(\gamma,2n)$ reaction and θ is the nuclear temperature of the intermediate residual nucleus.

Then

$$\theta=[(E-E_n)/a]^{1/2},$$

and

$$\epsilon_c=E-E_{2n},$$

where E_n and E_{2n} are the thresholds for the (γ,n) and $(\gamma,2n)$ reactions, and a is the level density parameter in units of MeV^{-1}. On applying Eq. (3) to the experimental data, the value for a was determined to be 17.1±0.5 MeV^{-1}. Values for the level density parameter obtained from (n,n') reaction studies[14] on Au have been obtained over a range from 3.4 to 18 MeV^{-1}. A more recent value reported is 17.1 (±20%).[15]

A Lorentz line with the following resonance parameters can be fitted to the formation cross section of Au. Peak cross section σ_0 is 535 mb at 13.90 MeV. Width at half maximum (Γ) is 4.2 MeV. The fit is good up to 25 MeV (Fig. 9).

[9] R. Nathans and J. Halpern, Phys. Rev. **93**, 437 (1954).
[10] R. Montalbetti, L. Katz, and J. Goldemberg, Phys. Rev. **91**, 659 (1953).
[11] I. C. Nascimento, G. Moscati, and J. Goldemberg, Nuclear Phys. **22**, 484 (1961).
[12] J. S. Levinger, *Nuclear Photodisintegration* (Oxford University Press, New York, 1960).

[13] J. M. Blatt and V. F. Weisskopf, *Theoretical Nuclear Physics* (John Wiley & Sons, Inc., New York, 1952), Chap. 8.
[14] D. B. Thompson, Doctoral thesis, University of Kansas, 1960 (unpublished).
[15] K. K. Seth (private communication); also Bull. Am. Phys. Soc. **7**, 23 (1962).
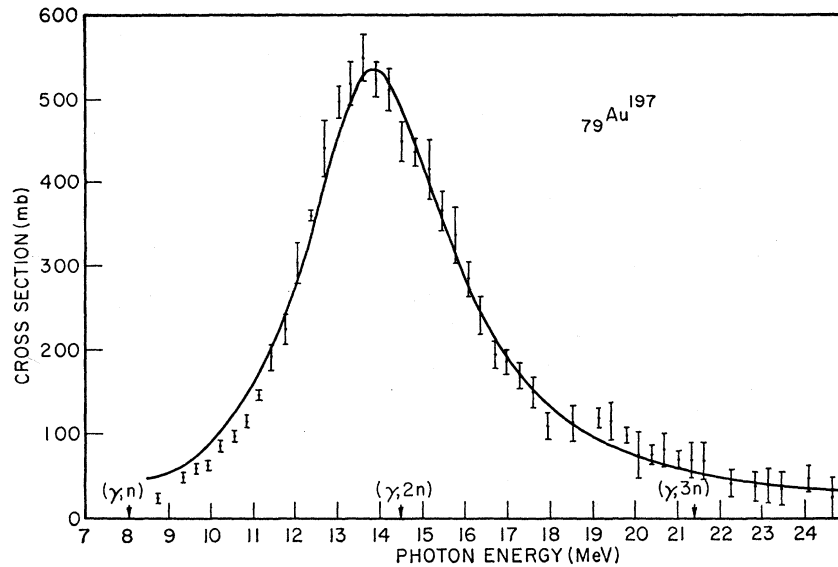
FIG. 9. The nuclear formation cross section for gold, consisting of $\sigma(\gamma,n)+\sigma(\gamma,2n)+\sigma(\gamma,np)$. The solid line is a Lorentz curve with a peak cross section of 535 mb at 13.90 MeV, and a width of 4.2 MeV.

The following summary represents the results obtained from the photonuclear measurements on Au. The experimental value of the integrated cross section was found to agree with the simple dipole-absorption sum rule, i.e., Eq. (1) with no correction for an exchange force. The "minus-second cross section," which is proportional to the nuclear polarizability, is also in agreement with the value derived from a simplified theoretical treatment, i.e., Eq. (2). For the derivation of Eq. (2), a nuclear radius parameter of $R_0 = 1.2$ F was used. Finally, the value for the nuclear level density parameter a agrees well with values determined from neutron scattering experiments. However, in evaluating a from the experimental data, the value used for the $(\gamma,2n)$ threshold was 15.20 MeV. This disagrees with the value of 14.47 MeV obtained from mass tables but corresponds to a linear extrapolation of the $\sigma(\gamma,2n)/\sigma_{tot}$ curve to the energy axis, as would be predicted by the evaporative model.

The narrow width Γ of the giant resonance at half-maximum, i.e., 4.2 MeV, does not indicate that any significant splitting due to a quadrupole moment is likely to be present. No effort was made, therefore, to fit more than one Lorentz line to the Au data, on the assumption that no significant or meaningful splitting is present and that the nucleus is essentially spherical.

ACKNOWLEDGMENTS